Cortical replay of ‘Time’ accompanied by hippocampal sharp-wave ripples

Xuanlong Zhu[a], Hongjie Jiang[b], Chenyang Li[c], Diogo Santos-Pata[a], ,Shaomin Zhang[c] , Zhaoxin Wang[d], Sze Chai Kwok[a]

[a]Division of Natural and Applied Sciences, Duke Kunshan University, Kunshan, Jiangsu, 215316, China
[b]Department of Neurosurgery, The Second Affiliated Hospital, School of Medicine, Zhejiang University, Zhejiang, 310003, China
[c]Qiushi Academy for Advanced Studies, Zhejiang University, Zhejiang, 310014, China
[d]Shanghai Key Laboratory of Brain Functional Genomics, School of Psychology and Cognitive Science, East China Normal University, Shanghai, China

Introduction

Replay has emerged as a pivotal mechanism in understanding how episodic memory is retrieved and consolidated. In this context, neural activity patterns are thought to either recapitulate past experiences or anticipate future events. While substantial evidence exists for the replay of "where" (location) and "what" (object) sequences in both rodents and humans, the "when" (time) aspect remains understudied. Given the inherent correlation between time and space, our study seeks to address this gap by isolating temporal information independently of visual content.

To this end, we employed intracranial electroencephalography (iEEG) data from epileptic human volunteers engaged in a temporal order judgment task. Participants were tasked with recalling the sequence of events in trial-unique videos. This design ensured that any observed replay could be attributed to the temporal structure rather than specific visual elements. After obtaining content-invariant time decoder from whole-brain neural representations and examining the temporal dependencies among reactivation through linear temporal modeling, we observed significant evidence supporting replay of time (temporal state) during both memory retrieval and subsequent resting periods. Our results suggest that time in episodic memory, like location ("where") and item ("what"), can be retrieved by a rapid replay mechanism, and our recollections of memory are not just holistic experiences but can be analyzed in terms of separate spatiotemporal context.

Method

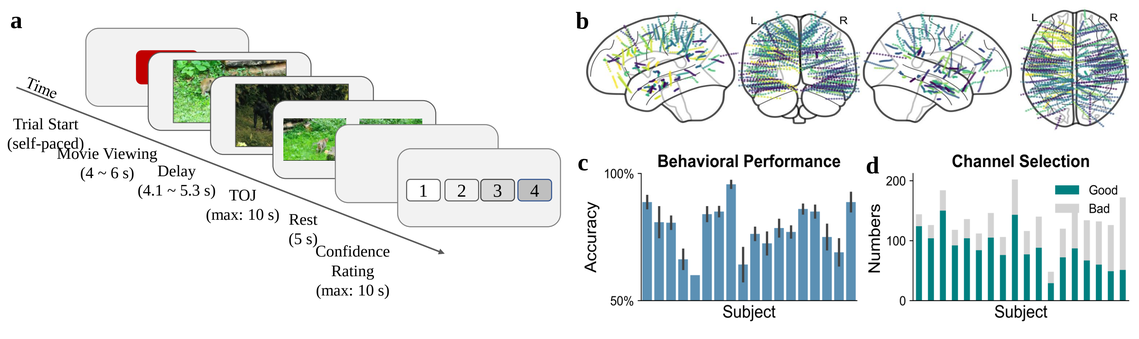

Fig 1. Experimental Design and Intracranial Data Acquisition

1a. Experimental paradigm. Each trial began with a 4~6 s clip of animals, categorized as either primates or non-primates. Participants were required to memorize the temporal order and select the earlier of the two presented images in later temporal order judgment (TOJ) phase. After the memory test, a 5-s rest period would be given during which no stimuli would be presented on the screen, and the participants would be instructed to blank out as much as possible.
1b. Recording locations. We collected approximate 2492 channels across 18 participants. Anatomical locations of all the implanted iEEG channels are shown in Montreal Neurological Institute (MNI) space. Marker colors are indicative of individual participants.
1c. Behavioral performance. Participants were screened with an average TOJ accuracy threshold above 50% and ordered by enrollment sequence. Error bars represent the standard error of the mean (SEM) across sessions for each participant.
1d. Channel Selection. In data preprocessing, channels located in the epileptic focus, nonparenchymal, or those deemed noisy by statistical measurement were excluded. Excluded channels were marked as "Bad Channels," while "Good" refers to the surviving channels.

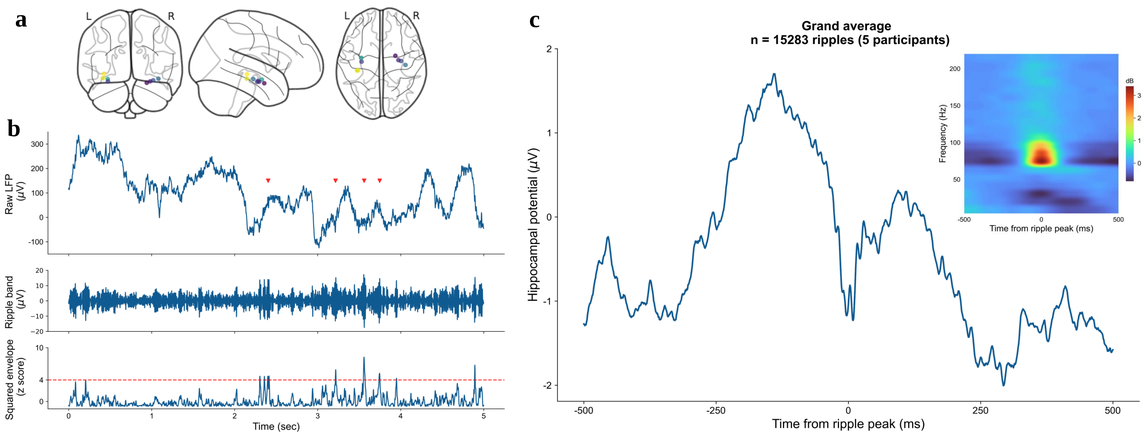

Fig 2. Sharp-wave ripple detection

2a. Anatomical Location. Hippocampal recording sites used for ripple detection is shown. Marker colors are indicative of individual participants (n = 5).
2b. SWR examples during recording. From top to bottom: raw LFP, ripple-band filtered LFP (70–180 Hz), and the normalized ripple-band envelope used for ripple detection. SWRs were defined as events above 4 SD.
6c. Grand average peri-ripple field potential and wavelet spectrogram centered on ripple peak (n = 15283 SWR events).

Result

Fig 3. Neural Coding of Time during the Encoding Period

3a. Decoding performance. Data from participants watching different videos were used to train the time decoders, which performed successfully. Testing on the same temporal states showed generally high accuracy, with errors mostly occurring between adjacent time states.
3b. State-to-state dissimilarity. The heatmap on the left shows the normalized Mahalanobis distance between neural representations of each temporal state, with warmer colors indicating greater dissimilarity. The right plot displays the normalized Mahalanobis distances across different lags. Dissimilarities accumulated over the state-to-state lags. Gray dashed lines on the background represent data from individual participant and the blue line indicates the group average.

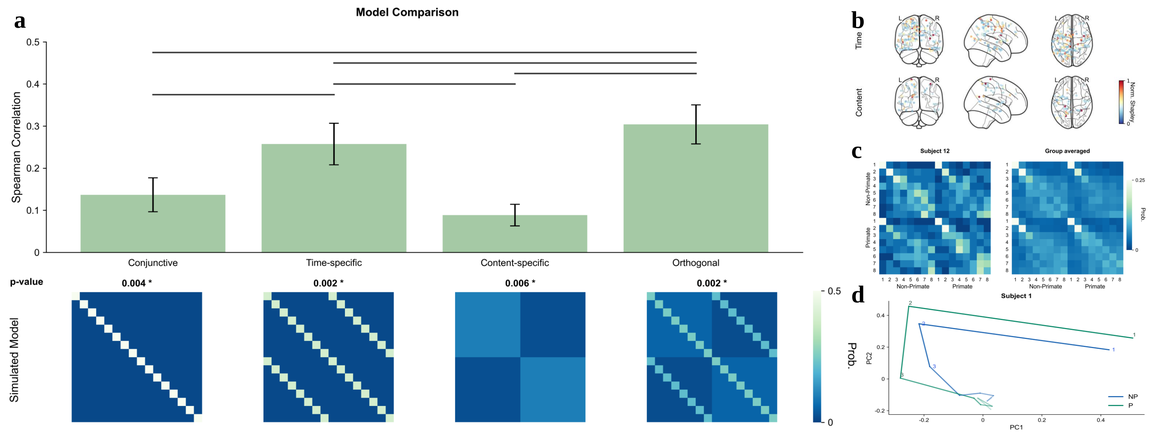

Fig 4. Disentangled neural representations of content and temporal journey

4a. Model comparison. The confusion matrices of the content-and-time decoders were modeled under four hypotheses: Conjunctive, Time-specific, Content-specific, and Orthogonal. Simulated matrices were shown in the bottom plot. Bootstrap tests showed that all models had significantly higher cosine similarity with the actual data compared to random data. Pairwise comparisons indicated the Orthogonal hypothesis was best supported, suggesting disentangled neural representations for content and time. Horizontal lines in the top plot indicate significant pairwise differences between hypotheses.
4b. Spatial distribution of features. The spatial distribution of normalized SHAP values shows the differences when the same feature set is used to decode content versus time. Time codes are more widely distributed, while content codes mainly rely on a few key features.
4c. Exemplar confusion matrices. Confusion matrices generated by the actual results of the content-and-time decoders are displayed: the left shows data from a single participant, while the right shows the group-averaged matrix. All data are row-normalized.
3d. PCA trajectory. Time code for different video types show similar temporal state trajectories in 2-D PCA space. Data are for illustration purpose only.

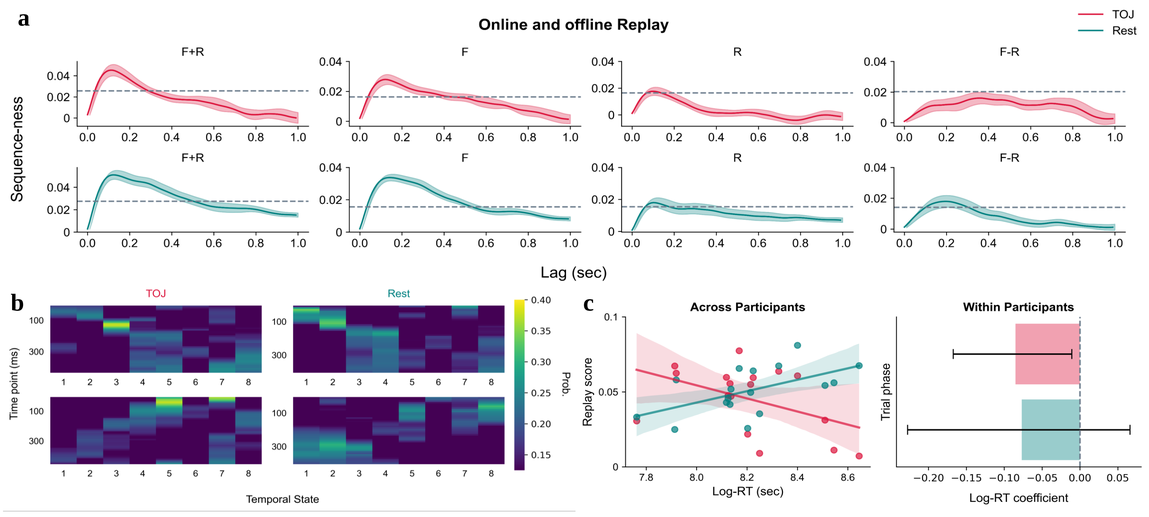

Fig 5. Bi-directional replay of temporal sequence

5a. On-task and off-task replay. Sequence-ness across different state-to-state lag are shown. Sequence-ness significantly higher than chancel level indicates replay of temporal sequence during the TOJ and post-retrieval Rest periods, with time lag peak at 120~130 ms. Significance was tested by circular shuffling the order of the temporal sequences 1000 times and calculating the maximum sequence-ness across all lags to generated a null distribution of sequence-ness. The threshold, represented by the dashed line in plot is set at the 95th percentile of the null distribution. Shaded areas represent SEM across participants.
5b. Replay event examples. Each cell in the heatmap represents the reactivation probability of a specific temporal state at given time points. In the top row, the temporal sequence is reactivated sequentially in the same order as the original experience, while in the bottom row, it is reactivated in reverse order. Data are from a single participant and are for illustration purposes only.
5c. Effect on memory performance. The effect of replay on memory was analyzed at two levels: a two-way ANOVA at the group level (left) and a mixed-effects linear model at the single-trial level (right). At the group level, there was a significant interaction between trial phase and RT, with on-task replay sequence-ness decreasing with longer RTs, and off-task replay sequence-ness increasing. At the single-trial level, only on-task replay sequence-ness showed a significant decrease with increasing RT. Error bars represent SEM across participants.

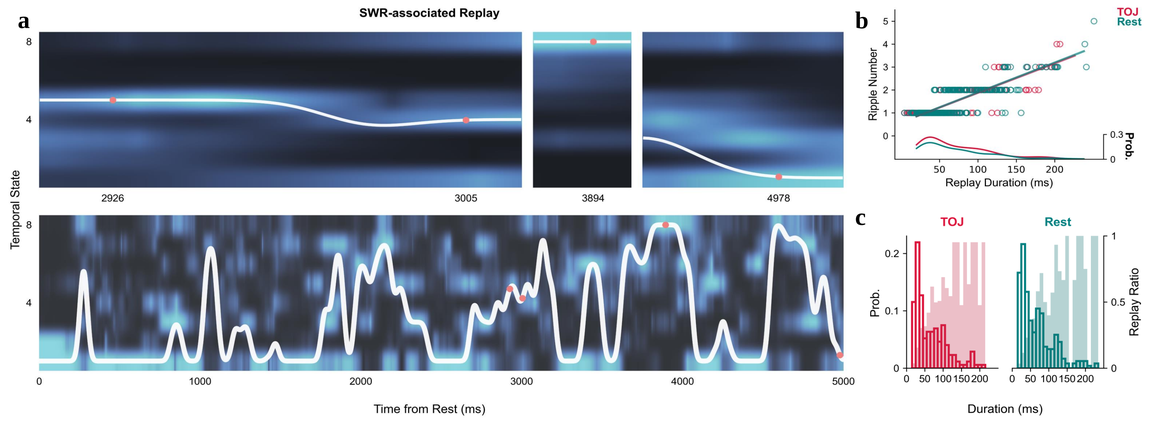

Fig 6. Hippocampal SWR-associated cortical replay

6a. Example of cortical replay events in a single trial with four hippocampal SWR.
The top panel illustrates the reconstructed temporal sequences accompanied by SWR burst (left) and isolated ripple (right). Read dots indicate the ripple peaks, arranged sequentially in chronical order. Heatmaps represent the reactivation level of each temporal state over time, with the white curves indicating the weighted average of temporal states.
6b. Extended replay. The line plot (top) shows the relationship between replay event duration and the corresponding number of ripples, along with the distribution of replay event durations (bottom).
6c. Replay accompanied by isolated ripples. Solid bars represent the distribution of hippocampal SWR durations, while shaded bars indicate the ratio of replay detected. Longer ripples are more likely to be accompanied by replay.

Summary

- Factorized Time code in human episodic memory.
- Bi-directional rapid replay of temporal sequence during both memory retrieval and subsequent resting.
- Distinct role of on-task and off-task replay in predicting memory performance.
- Similar to hippocampal replay, cortical replay is accompanied by hippocampal SWRs, not only in isolated events but also spanning multiple adjacent SWRs.